Current Topics in Pharmacology
Vol. 20, 2016

Original Communication

Antiproliferative effects of neuroprotective drugs targeting big Ca^{2+}-activated K^+ (BK) channel in the undifferentiated neuroblastoma cells

Angela Curci[1], Fatima Maqoud[1,3], Antonietta Mele[1], Michela Cetrone[4], Mariacristina Angelelli[1], Nicola Zizzo[2] and Domenico Tricarico[1,*]

[1]Department of Pharmacy, Pharmaceutical Sciences, University of Bari, Italy;
[2]Department of Veterinary Medicine, University of Bari, Italy.
[3]Faculty of Science, Chouaib Doukkali, El Jadida, Morocco.
[4]Istituto Tumori Giovanni Paolo II, IRCCS, National Cancer Institute, Bari, Italy.

ABSTRACT

The big Ca^{2+}-activated K^+ (BK) channel has a role in regulating cell viability and survival in a variety of cells. The effects of drugs targeting the BK channels in neuronal and smooth muscle tissues in the human SH-SY5Y cell and mouse Neuro2A undifferentiated neuroblastoma cells have never been investigated. The expression/activity of BK channel subunits and the effects of the BK channel openers: acetazolamide (ACTZ) (10^{-7} - 2 x 10^{-4} M), resveratrol (RESV) (10^{-7} - 2 x 10^{-4} M), dichlorphenamide (DCP) (10^{-12} - 2 x 10^{-4} M), bendroflumethiazide (BFT) (10^{-9} - 10^{-5} M) and riluzole (RIL) (10^{-6} - 10^{-4} M) were evaluated by real time-polymerase chain reaction (RT-PCR)/patch-clamp experiments in SH-SY5Y cells and Neuro2a. Cell proliferation was evaluated by cell-dehydrogenase activity (CCK8-assay), cell impedentiometric (Scepter-counter) and clonogenic assays. An elevated expression/activity of the hslo1-BK channel subunit was observed in the SH-SY5Y, while a low expression/activity of this subunit was found in the Neuro2a. Tetraethylammonium (TEA) (1 - 5 x 10^{-3}) and iberiotoxin (IbTX) (10^{-9} - 6 x 10^{-7} M) caused a marked inhibition of the whole-cell K^+-currents in SH-SY5Y. A mild inhibition of the K^+-currents was found in Neuro2a with these compounds. The application of ACTZ, DCP, RESV and BFT to the patches failed to activate the K^+-currents but rather reduced it. The rank order of efficacy of the drugs as K^+-current inhibitors at +30 mV (Vm) was: TEA > RESV $\geq$ IbTX > DCP > ACTZ > BFT. RESV and IbTX irreversibly reduced the K^+-currents and the cell number in the enzymatic, clonogenic and impedentiometric assays with RESV being more effective than IbTX. TEA reversibly reduced the K^+-currents without affecting cell proliferation. Whereas, RIL potentiated the BK current and reduced cell-dehydrogenases activity with no changes in the cell morphology and number. The observed irreversible BK channel-blocking action exerted by RESV and IbTX can be associated with anti-proliferative effects in cells overexpressing hslo1-BK channel subunit. This can be an additional mechanism contributing to the cytotoxic action of RESV in SH-SY5Y cells.

KEYWORDS: cell number, voltage-dependent potassium channels, patch-clamp, neuroblastoma cells, big calcium-activated potassium channels

ABBREVIATIONS

SH-SY5Y : human neuroblastoma cell line
Neuro2a : mouse neuroblastoma cell line

*Corresponding author: domenico.tricarico@uniba.it

Kv	:	voltage-dependent potassium channels
BK	:	big conductance calcium-activated potassium channels
SK	:	small conductance calcium-activated potassium channels
CDA	:	cell dehydrogenases activity
4-AP	:	4-aminopyridine
TEA	:	tetraethylammonium
MS	:	multiple sclerosis
ASL	:	amyotrophic lateral sclerosis
RIL	:	riluzole
ACTZ	:	acetazolamide
RESV	:	resveratrol
DCP	:	dichlorphenamide
BFT	:	bendroflumethiazide
DMSO	:	dimethyl sulfoxide

INTRODUCTION

The big calcium-activated K^+ (BK) channels play a role in the basic cellular processes such as electrical excitability of cell membrane, thereby regulating smooth muscle tone, skeletal muscle plasticity, K^+ ion levels, neurotransmitter release and cell proliferation [1-9].

The BK channel openers are small synthetic compounds, natural compounds and marketed drugs showing a variety of actions in smooth muscle, neuronal and skeletal muscle tissues [10-15]. Acetazolamide, riluzole and resveratrol show neuroprotective effects in animal model of diseases as well as in human patients. These drugs are also capable of opening the BK channels at therapeutic concentrations in different tissues including neurons. Acetazolamide is a pan-carbonic anhydrase inhibitor successfully used in the treatment of periodic paralysis, ataxia and in some forms of epilepsy [16-19]. Riluzole is prescribed in the treatment of the multiple sclerosis and amyotrophic lateral sclerosis. This drug acts by opening the small conductance K^+ (SK) channel and BK channel, blocking the voltage-dependent Na^+ and N/P/Q-type Ca^{2+} channels, inhibiting glutamatergic signalling and protein kinase C activity [20-23]. Resveratrol exerts cytoprotection against neurodegeneration through a variety of transducer molecules and ion channels including BK channels in neurons and vascular smooth muscle cells [24-26].

In addition, acetazolamide, riluzole and resveratrol may show anti-proliferative actions in some cancerous cells. Acetazolamide for instance inhibits the CAIX in hypoxic tumour with a change in the intra/extra cellular H^+ concentration slowing down the tumour progression [27]. Acetazolamide has been tested with some efficacy in many tumors like bronchial carcinoid, renal carcinoma cells, breast cancer cells, colon cancer cells, bladder cancer, glioblastoma, and gastric carcinoma [28]. Anti-proliferative effects were also observed with riluzole in melanoma as well as in other cancers associated with glutamatergic oncogenes [29]. Resveratrol affects cell growth, apoptosis, angiogenesis and invasion through a variety of death signalling cascades [30]. This drug of natural origin showed some efficacy *in vivo* on breast, colorectal, liver, pancreatic, and prostate cancers [31]. Emerging evidence suggests that resveratrol may also exert cytotoxic action in neuroblastoma cells down-regulating the AKT signalling in the micromolar concentration range [32].

Despite their neurological and anti-proliferative effects, no data are available on the effects of acetazolamide and riluzole on neuroblastoma cells; furthermore the role of BK channel in the anti-proliferative effects of resveratrol has never been investigated.

In the present work, the expression/activity of the BK channel and response to drugs were evaluated by RT-PCR and patch-clamp experiments in the human SH-SY5Y and mouse Neuro2A neuroblastoma cells. The effects of acetazolamide and its structurally related analogues dichlorphenamide and bendroflumethiazide, and the effects of resveratrol and riluzole on cell proliferation were investigated in the neuroblastoma cells using the impedentiometric based assay which is an index of ion channel activity and electrogenic transporters [8]. The drug effects on cell-mitochondrial dehydrogenases activity (CDA) and on the clone formation were evaluated by enzymatic colorimetric and clonogenic assays, respectively.

MATERIALS AND METHODS

Drugs and solutions

In whole-cell patch-clamp experiments, the pipette (intracellular) solution contained (10^{-3} M):

132 K^+-glutamate, 1 ethylene glycol-bis (β-aminoethylether)-N, N, N, N-tetraacetic acid (EGTA), 10 NaCl, 2 $MgCl_2$, 10 HEPES, 1 Na_2ATP, and 0.3 Na_2GDP, pH = 7.2 with KOH. The bath (extracellular) solution contained (10^{-3} M): 142 NaCl, 2.8 KCl, 1 $CaCl_2$, 1 $MgCl_2$, 11 glucose, and 10 HEPES, pH = 7.4 with NaOH. $CaCl_2$ was added to the pipette solutions to give free Ca^{2+} ion concentration of 1.6 x 10^{-6} M in whole-cell experiments. The calculation of the free Ca^{2+} ion concentration in the pipette was performed using the Maxchelator software (Stanford Univ., USA). The compounds under investigation were the following: acetazolamide (ACTZ) (10^{-7} - 2 x 10^{-4} M), dichlorphenamide (DCP) (10^{-12} - 2 x 10^{-4} M), bendroflumethiazide (BFT) (10^{-9} - 10^{-5} M), resveratrol (RESV) (10^{-7} - 2 x 10^{-4} M), 4-aminopyridine (4AP) (10^{-10} - 10^{-4} M), riluzole (RIL) (10^{-6} - 10^{-4} M), dimethyl sulfoxide (DMSO) (8.4 x 10^{-10} - 1.7 x 10^{-1} %), iberiotoxin (IbTX) (10^{-9} - 6 x 10^{-7} M), apamin (2 x 10^{-7} M), glibenclamide (1, 100 x 10^{-9} M) and diazoxide (250 x 10^{-9}, 200 x 10^{-6} M). Tetraethyl-ammonium chloride (TEA) (1 - 5 x 10^{-3}) and barium chloride (Ba^{2+}) (1 - 5 x 10^{-3}) were used to determine leak current in patch-clamp experiments. All reagents were purchased from Sigma (SIGMA Chemical Co., Mi, Italy). Stock solutions of the drugs under investigation were prepared by dissolving the drugs in DMSO at the concentration of 118.6 x 10^{-3} M. TEA was dissolved in DMEM+ or bath solution. Microliter amounts of the stock solutions were then added to the bath solution or cell culture medium, as needed. Therapeutic drugs are often formulated using DMSO that favours dissolution of molecules in the physiological medium [33, 34].

Cell culture

The human neuroblastoma cell line SH-SY5Y (ATCC® CRL2266™) and mouse Neuro-2a (ATCC® CCL-131™) were purchased from American Type Culture Collection (ATCC, Manasass, Virginia, USA). The cells were cultured in Dulbecco's Modified Eagle's Medium (DMEM) supplemented with 10% foetal bovine serum (FBS), 1% L-glutamine and 1% antibiotics in a humidified atmosphere containing 5% CO_2. All culture medium components were purchased from EuroClone (EuroClone S.p.A., Mi, Italy). The experiments were performed on undifferentiated cells at passage 4, 10 and 14 during the experiments. Cells were maintained in an undifferentiated stage by culturing them in plastic plates in the absence of NGF, IGF1 or retinoic acid, which are known to induce differentiation [35]. The morphological assessment of the stage of differentiation involved monitoring the cells over 72 hours to detect the extension of long neuritis from the cell body. A differentiated cell was defined as a cell with a neuritis length greater than the cell body of the individual cell (on average greater than 10 μm in length). Plates showing a large number of differentiated cells based on neuritis length were discarded from the experiments.

Patch–clamp experiments

The native K^+-currents were recorded in the SH-SY5Y and Neuro2a cells during +20 mV (Vm) voltage steps, in the range of potentials going from -150 mV (Vm) to +110/+150 mV (Vm), starting from HP = -60 mV (Vm), in the presence of internal Ca^{2+} ions, in asymmetrical K^+ ion concentrations (intracellular K^+: 132 x 10^{-3} M; extracellular K^+: 2.8 x 10^{-3} M) using patch-clamp technique [8, 36-39]. The resulting K^+-currents were leak subtracted. Leak current was measured after adding saturating concentration of an external solution containing Ba^{2+} ions (5 x 10^{-3} M) and TEA (5 x 10^{-3} M) which caused a full block of Kir, Kv and BK channels. Drug effects were investigated in a physiological range of potentials going from -80 mV (Vm) to +30 mV (Vm) for all drugs. The K^+-currents were recorded at 20 °C and sampled at 2 kHz (filter = 1 kHz) using an Axopatch-1D amplifier equipped with a CV-4 headstage (Axon Instruments, Foster City, CA).

Current analysis was performed using pClamp 10 software package (Axon Instruments). The criteria for accepting the data entry was based on the stability of the seal evaluated by observing the noise levels not exceeding 0.6 pA. The resistance of the pipettes were 9 ± 0.2 MΩ (Number of pipettes = 220). The cells were exposed to the drug solutions for 1 min before recordings. In patch clamp experiment, the bath solution was tested against K^+-currents in the absence (control) and presence of DMSO, and in the presence of DMSO+drug. Increasing concentrations of drug

solutions were applied to the cells by the fast perfusion system (AutoMate, Sci. Berkeley, California 94710 USA). No more than six different solutions were applied to the same cell. Seal resistance was continuously monitored during patch solution exchange.

Cell transfection

Transfection was performed following the siRNA transfection protocol for Lipofectamine 2000 (Qiagen, KJ Venlo, NL, USA). Briefly, 40000 SH-SY5Y cells were plated in six-well plates (Falcon, Becton-Dickinson) one day before transfection. The transfection was performed in OPTI-MEM (Invitrogen) for 4 h. The transfection mixture contained 5 ml of siRNA and Lipofectamine, each, in a total of 3 ml OPTI-MEM. After 4 h, the transfection mixture was replaced by OPTI-MEM þ 10% FCS. The siRNA sequence targeting the KCNMA1 gene was: gtgggtctgtccttccctact. Experiments were performed after 3 days from the transfection.

RT-PCR experiments

A 100 mm Petri dish containing a 7 x 106 cell was treated with trypsin and centrifuged at 10.000 x g for 5 minutes, the cell pellet was washed with Nuclease-Free Water (life technologies C.N. AM9930), and stored at -80 °C. For each sample, total RNA was isolated by RNeasy Fibrous Tissue Mini Kit (Quiagen C.N. 74704) and quantified by using a spectrophotometer (ND-1000 Nano- Drop, Thermo Scientific) [40].

RT–PCR was performed using the LightCycler system and the LightCycler® FastStart DNA Master Hybridization Probe kit (Roche Diagnostics). Primers for G6PD and KCNMA1 hybridization products were obtained from TIB MolBiol (Berlin, BRD). PCR primers were: KCNMA1: KCNMA1_s: cctggcctcctccatggt, KCNMA1_a: ttctgggcctccttcgtct, G6PD: G6ex7,8 R ttctgcatcac gtcccgga, G6ex6 S accactacctgggcaaggag. Hybridization probes were: KCNMA1: KCNMA1_fl: agcgtccgccagagcaagat, KCNMA1_lc: atgaagagg cccccgaagaaagt, G6PD: G6ex_FL: cagatggggccgaa gatcctgtt, G6ex_LC: caaatctcagcaccatgaggttctgcac. PCR conditions were: activation: 10 min 951C PCR cycle: 5 s at 951C, annealing 5 s at 571C, elongation 15 s at 721C, 40 cycles. Raw data for KCNMA1 expression were corrected by comparison to the related G6PD controls. These corrected values were compared to each other to obtain a relative expression.

To perform reverse transcription, for each sample, 400 ng of total RNA was added to 1 µl dNTP mix 10 mM each, (Roche N.C. 11277049001), 1 µl Random Hexamers 50 µM (life-technologies C.N. n808-0127) and incubated at 65 °C for 5 min. Afterwards, 4 µl 5X First Standard Buffer (life-technologies C.N. Y02321), 2 µl 0,1 MDTT (life-technologies C.N. Y00147) and 1 µl Recombinant RNasin Ribonuclease Inhibitor 40 U/µl (Promega, C. N. N2511) were added and incubated at 42 °C for 2 min. For each solution 1 µl Super Script II Reverse Transcriptase 200 U/µl (life-technologies C.N. 18064-014) was added and incubated at 25 °C for 10 min, at 42 °C for 50 min and at 70 °C for 15 min. 5 µl of the reverse transcription mix was used for PCR reaction with 12.5 µl of PCR master mix (Promega C.N. M7502) 0.5 µM of each primer (upstream and downstream) for a final volume of 25 µl. The primer pair used to amplify each gene is reported in table 1.

PCR conditions: step 1: 95 °C for 2 min; step 2: 95 °C for 1 min; step 3: 51 °C - 60 °C for 1 min; step 4: 72 °C for 1 min; and step 5: 72 °C for 5 min; steps 2 and 4 were repeated 35 times. The experiments were conducted as previously described [40, 41].

Impedentiometric assay

Measures of cell number and morphology were based on the relationship existing between voltage changes and cell volume changes by using the Scepter™2.0 cell counter (MERK-Millipore, USA) which is equipped with 60 µm and 40 µm sensors; in our experiments we used the 60 µm sensor for particles between 6 µm and 36 µm. The cell volume regulation is under control of ion channels and transporters of the surface membrane and is associated with cell death [8].

Intracellular dehydrogenases activity assay

The activity of intracellular dehydrogenases was assessed by using the Cell Counting Kit-8 (CCK-8) (Enzo Life Sciences International, Inc, USA) which utilizes highly water-soluble tetrazolium salt. WST-8 2-(2-methoxy-4-nitrophenyl)-3-(4-nitrophenyl)-5-(2,4-disulfophenyl)-2H-tetrazolium,

Table 1. Primers used for PCR reaction.

Primer name	Nucleotide sequence (5'-3')	Annealing temperature
KCNMA1-C1-For	TGACATCACAGATCCCAAAA	52
KCNMA1-C1-Rev	CGAGGTGTTGGGTGAGTTCC	52
KCNMB1-For	GTGAAGTCATTGCCTGCTCA	58
KCNMB1-Rev	GGAGAACTCAGGCACAGAGG	58
KCNMB2-For	CACTGAAGGCAGGAGAGGAC	58
KCNMB2-Rev	CAGTCTGGACCACAGCTGAA	58
KCNMB3-For	CTAGGTGGTGCCCTGATTGT	58
KCNMB3-Rev	TCTTCCTTTGCTCCTCCTCA	58
KCNMB4-For	TCCTGACCAACCCCAAGTGC	58
KCNMB4-Rev	AAGCAATGCAGGAGGACAAT	58

monosodium salt produces a water-soluble formazan dye upon reduction in the presence of an electron carrier. It is reduced by dehydrogenases in cells to give an orange coloured product (formazan), which is soluble in the tissue culture medium. The detection sensitivity of CCK-8 is higher than other tetrazolium salts [42]. The cells were seeded in 96-well plates at a density of 6.5 x 10^3 cells/well with 100 µL of DMEM+ per well and pre-incubated for 24 h in a humidified incubator. On the next day, different concentrations of the drug solution was added into the culture medium in wells. Each drug solution was obtained by diluting the drug stock solutions in DMSO with DMEM+. After incubation for an appropriate time (3 h, 6 h or 24 h), 10 µL of CCK8 solution was added to each well. The absorbance at 450 nm was measured after 2 h incubation with CCK-8 solution, using a microplate reader (Victor 3V PerkinElmer). All experiments were performed in triplicates. The data were expressed in comparison with DMSO condition or control.

Clonogenic survival assay

The clonogenic survival assay was performed according to the protocol previously described by Franken with some modifications [43]. Briefly, 100 cells evaluated by Scepter™2.0 cell counter were plated before treatment in 60 mm dishes. After allowing time for the cells to attach to the dish (24 h), the effects of different concentrations of the drugs and DMSO 8.4 x 10^{-3} % (v/v) on the number of colonies were investigated after 3 hours and 6 hours of incubation time. Control cells were grown in the absence of drugs and treated with equivalent volumes of DMEM+. Each experimental condition was performed in triplicates. At the end of the incubation period, the culture medium was carefully replaced by DMEM+ and the cells were cultured for 2 weeks. Upon termination of the assay, the cells were washed with phosphate buffered saline (PBS) and the colonies formed were subsequently fixed with 10% v/v formaldehyde for 2 hours at room temperature and stained with 0.5% v/v crystal violet overnight. Then, the dishes were rinsed with water and air-dried. Colonies were counted and analyzed by using an OpenCFU program [44].

Data analysis and statistics

The data were collected and analyzed using Excel software (Microsoft Office 2010). Data are expressed as mean ± S.E. unless otherwise specified.

The concentration-response relationships of the drugs under investigation could be fitted with the following equation:

$$(I_{drug} - I_{leak}) / (I_{control\ or\ DMSO} - I_{leak}) \times 100 - 100 = Emax / (1+(DE50/[Drug])^n)$$

I_{drug} is the K^+-current recorded at +30 mV in the presence of a specific concentration of the compound under study; I_{leak} is the current recorded at

+30 mV in the presence of saturating concentrations of TEA and Ba^{2+} ions at 5 x 10^{-3} M concentration; I control or DMSO is the K^+-current recorded at +30 mV in the absence of drugs; Emax represents the maximum inhibitory or activating effect of drug under investigation, in the range of tested concentrations; DE50 is the concentration of drug needed to inhibit or activate the current by 50%; [Drug] is the concentration of the drug considered; *n* is the slope factor of the curve. The algorithms of the fitting procedures used are based on a Marquardt least-squares fitting routine. Data analysis and plots were performed using SigmaPlot software (Systat Software, Inc., San Jose, CA).

The % change in the cell dehydrogenases activity induced by the drugs, and the cell number was calculated with respect to the control condition or with respect to the DMSO condition using the following equation:

$$\% \text{ change of the cell dehydrogenases activity} = \frac{(\text{ABS exp. condition})}{(\text{ABS control or DMSO})} \times 100 - 100$$

$$\% \text{ change of the cell number} = \frac{(\text{N cells exp. condition})}{(\text{N cells control})} \times 100 - 100$$

Experimental condition represents the incubation of cells with the drugs under investigation at a specific concentration over a period of 3 h, 6 h or 24 h; control refers to the incubation of cells in the presence of DMEM+ or DMEM+ and DMSO used as a co-solvent in the same aliquot of the drug solution; ABS is the mean absorbance of the three repetitions.

The plating efficiency (PE) and the surviving fraction (SF) were evaluated using the clonogenic cell number assay and calculated using the following equation:

$$PE\ (\%) = \frac{\text{N of colonies formed}}{\text{N of cells seeded}} \times 100$$

$$SF = \frac{\text{N of colonies formed after treatment}}{\text{N of cells seeded} \times PE}$$

Linear regression analysis based on the following equation: $y = ax + b$ was used for the calculation of the coefficient of correlation (R) between variables.

Differences within and between drug treatment groups were evaluated using one way analysis of variance (ANOVA) in cell number assays, and Bonferroni correction was used to counteract for multiple comparisons and test for the significance of each individual hypothesis at a significant level of $\alpha = 0.05$.

Student t-test, at $p < 0.05$ and $p < 0.001$ levels of significance, was used to test for significance between means.

RESULTS

Effects of Kv/BK channel modulators on K^+ currents recorded in SH-SY5Y and Neuro2a cells

A large whole-cell K^+-current was recorded in asymmetrical K^+ ion concentrations (intracellular K^+: 132 × 10^3 M; extracellular K^+: 2.8 × 10^{-3} M) and internal free Ca^{2+} ions of 1.6 × 10^{-6} M concentration in the SH-SY5Y at cell culture passage 10 (Table 2); similar data were obtained at cell passages 4 and 14. In contrast, a significantly lower whole-cell K^+-current amplitude was recorded in the same experimental condition in the Neuro2a at cell culture passage 10 with respect to that recorded in the SH-SY5Y cells (Table 2); similar data were obtained at cell culture passages 4 and 14. The reversal potential of the current in Neuro2a calculated from the intercept of the current-voltage relationship was -40.5 ± 4 mV (Number of cells = 32) suggesting that the current was K^+ ion-selective. The whole-cell K^+-current of Neuro2a cells were mildly affected by IbTX (6 x 10^{-7} M) and RESV (10^{-4} M) (Table 2), while the unselective BK/Kv blocker TEA (1 x 10^{-3} M) (Number of cells = 12) reduced the whole-cell K^+-current by -71.2 ± 14%.

The pharmacological characterization of the K^+-current was therefore performed in the SH-SY5Y cells. This current was reduced respectively by -12.7 ± 5%, -15.8 ± 3%, -67 ± 8% and -95.8 ± 9% following the application of the SK channel blocker apamin (2 x 10^{-7} M), the Kv4 blocker 4AP (5 x 10^{-4} M), the BK blocker IbTX (6 × 10^{-7}) and TEA (1 x 10^{-3} M) (Number of cells = 21) (Figure 1).

The application of ACTZ (10^{-7} - 2 x 10^{-4} M) (Number of cells = 12), BFT (10^{-9} - 10^{-5} M)

Table 2. Expression/activity of the BK channel alpha subunits in SH-SY5Y and Neuro2a neuroblastoma cells and in SH-SY5Y cells after transfection with siRNAm against KCNMA1, and response to IbTX and RESV.

	Neuro2a (cell passage 10)	SH-SY5Y (cell passage 10) 3 days after transfection with siRNAm against KCNMA1	SH-SY5Y control cell (cell passage 10)
h-slo1 expression/K^+-current (pA/pF)	1.41 ± 0.01/140.3 ± 12 (N plates/N cells =3/25)	1.22 ± 0.1*/111.3 ± 31* (N plates/N cells = 3/24)	3.42 ± 0.3/350.3 ± 34 (N plates/N cells = 3/28)
		IbTX (6×10^{-7} M)	
K^+-current inhibition (%)	-11.2 ± 3 (N cells = 25)	-1.2 ± 7* (N cells = 24)	-53.3 ± 9° (N cells = 24)
Change in cell number (%) after 6 h of incubation:			
Impedentiometric assay	+21.2 ± 9 (N plates = 3)	+2.2 ± 1* (N plates = 3)	-48.2 ± 9° (N plates = 3)
Cell-dehydrogenase assay	+11.1 ± 3 (N plates = 3)	-9.1 ± 5* (N plates = 3)	-49.3 ± 11° (N plates = 3)
		RESV (10^{-4} M)	
K^+-current inhibition (%)	-12.2 ± 6 (N cells = 25)	-11.3 ± 5* (N cells = 24)	-71.5 ± 6° (N cells = 24)
Change in cell number (%) after 6 h of incubation:			
Impedentiometric assay	-28.2 ± 4° (N plates = 3)	-21.3 ± 5*,° (N plates = 3)	-58.2 ± 9° (N plates = 3)
Cell-dehydrogenase assay	-27.1 ± 3° (N plates = 3)	-24.1 ± 6*° (N plates = 3)	-59.3 ± 12° (N plates = 3)

*Data significantly different with respect to the data from control SH-SY5Y cells by student t- test $p < 0.05$.
°Data significantly different with respect to the control data by student t- test $p < 0.05$.

(Number of cells = 6), RESV (10^{-7} - 2 x 10^{-4} M) (Number of cells = 5), DCP (10^{-12} - 2 x 10^{-4} M) (Number of cells = 9) to SH-SY5Y cells reduced the whole-cell K^+-currents in the presence of DMSO and no activating actions were observed in this cell line with these drugs (Figure 2A). 4AP (10^{-10} - 5 x 10^{-4} M) was a weak inhibitor of the K^+ channel current in our experiments (Number of cells = 5). TEA (5 x 10^{-3} M) and Ba^{2+} (5 x 10^{-3} M) ions fully inhibited the whole-cell K^+-currents in the absence of DMSO (Figure 2A).

The application of DMSO (8.4 x 10^{-10} - 1.7 x 10^{-1} %) to SH-SY5Y cells tested at the percentage concentrations (v/v) corresponding to the amount used as a co-solvent caused a non-significant decrease in K^+-currents with respect to that of the controls recorded at +30 mV (Vm) (DMSO *vs* control, student t test $p > 0.05$) (Figure 2A).

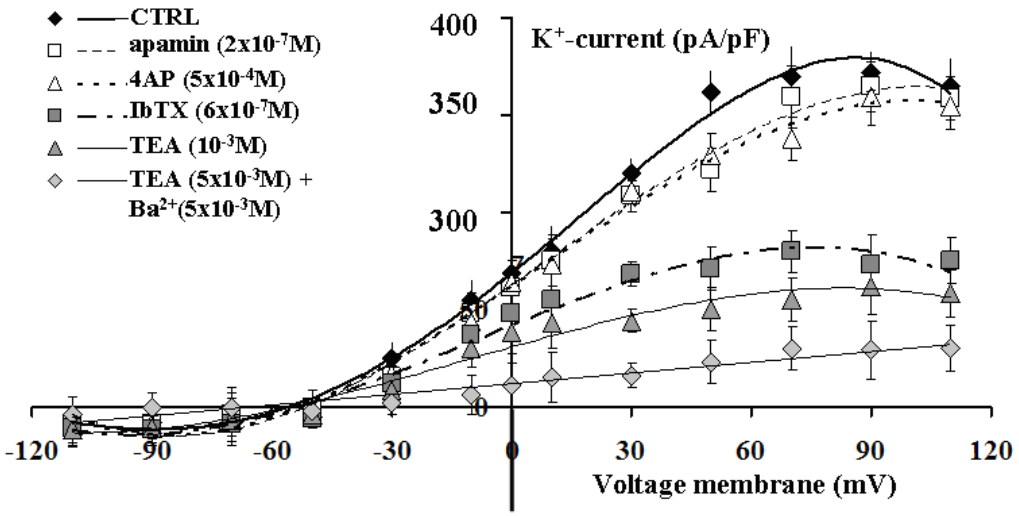

Figure 1. K^+-currents in human SH-SY5Y neuroblastoma cells (cell culture passage 10). The current/voltage relationship was recorded in the absence (CTRL) or in the presence of apamin (2 x 10^{-7} M), 4-aminopyridine (4AP) (5 x 10^{-4} M), iberiotoxin (IbTX) (6 x 10^{-7} M), tetraethylammonium (TEA) (1 x 10^{-3} M) and TEA (5 x 10^{-3} M) + Ba^{2+} ions (5 x 10^{-3} M) (Number of cells = 8). The K^+-currents were recorded in a whole-cell configuration in physiological K^+ ion concentrations. The whole-cell patches were perfused with each solution enriched with the drugs for 1 min before recording. The BK blocker IbTX and the unselective Kv blocker TEA were the most effective inhibitors.

ACTZ, BFT, RESV and 4AP reduced the whole-cell K^+ currents of SH-SY5Y cells in a concentration-dependent manner however showing different efficacies (Figure 2B). RESV, ACTZ, DCP, BFT and 4AP showed a maximal efficacy to inhibit the K^+-current respectively, of -68 ± 3%, -40 ± 5%, -40.1 ± 4%, -28 ± 3% and -15 ± 7%. The DE50 of RESV, ACTZ, BFT and DCP to inhibit the K^+-current was 2.29 x 10^{-6} M (slope = 0.27), 1.46 x 10^{-7} M (slope = 0.47), 1.81 x 10^{-7} M (slope = 0.37) and 1.2 x 10^{-9} M (slope = 0.87), respectively; it was not possible to calculate this parameter for 4AP. A variance ratio F of 2.2 within and between groups was calculated suggesting a statistical difference between concentration-response data which was due to the RESV data (ANOVA one way $F = 2.2$, $p < 0.05$; Bonferroni's $p < 0.05$).

In order to evaluate the contribution of the IbTX-sensitive current to the observed RESV effects, the SH-SY5Y cells were exposed to a combined treatment of IbTX and RESV. The application of RESV (2 x 10^{-4} M) solution to the cells in the presence of IbTX (6 x 10^{-7} M) caused a mild non-significant additional reduction of K^+-channel currents with respect to that observed in the presence of IbTX alone (Number of cells = 5) (ANOVA one way $F = 1.1$, $p > 0.05$) (Figure 3).

We found that a washout period of 6 min of RESV (10^{-4} M) solution failed to restore the K^+-current in SH-SY5Y cells (Figure 4). A washout period of RESV (10^{-4} M) solution > 6 min failed to restore the K^+-currents to the controls (Number of cells = 6) (data not shown). Similarly, IbTX (6 x 10^{-7} M) in the same experimental condition caused an irreversible reduction in the K^+-current (Figure 4). In contrast, the K^+-current was almost fully restored to the controls after 30 s of washout of TEA solution (10^{-3} M) (Figure 4). In the control condition, the K^+-currents were stable all over the period of observations 0-6 min (Figure 4). The percent changes in the K^+ currents after 6 min of washout of drug solutions calculated at +30 mV (Vm) was: -4.25 ± 1 (Number of cells = 6), -4.08 ± 0.9 (Number of cells = 5), -65.8 ± 6 (Number of cells = 6) and -59.7 ± 9 (Number of cells = 5) following the cell treatments to control, TEA (10^{-3} M) (TEA *vs* control, t test $p > 0.05$), RESV (2 x 10^{-4} M) (RESV *vs* control, t test $p < 0.05$) and IbTX (6 x 10^{-7} M) (IbTX *vs* control, t test $p < 0.05$) solutions, respectively.

RIL (10^{-6} - 10^{-4} M) (Number of cells = 26) induced a concentration-dependent activation of the K^+-currents of SH-SY5Y cells at +30 mV (Vm)

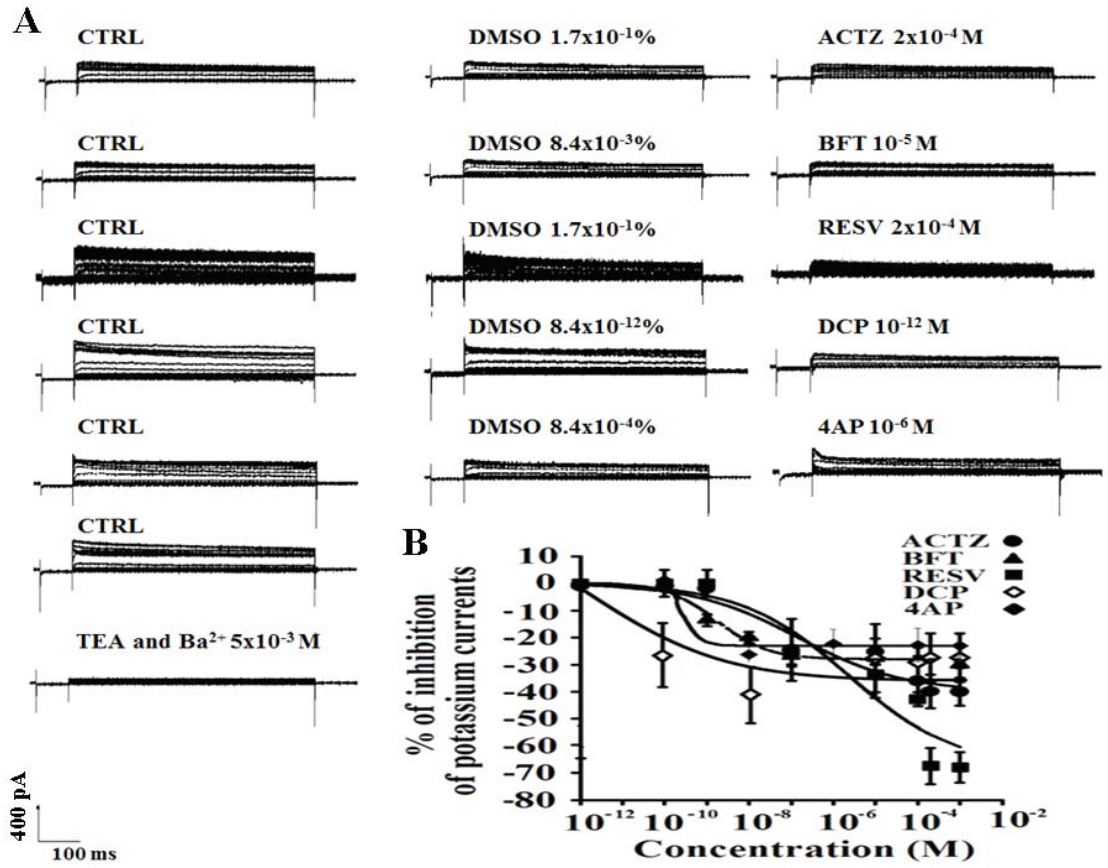

Figure 2. Effects of acetazolamide (ACTZ), bendroflumethiazide (BFT), resveratrol (RESV), dichlorphenamide (DCP), 4-aminopyridine (4AP) and DMSO on whole-cell K^+-currents in human SH-SY5Y neuroblastoma cells (cell culture passage 10). **(A)** Sample traces of K^+-currents recorded in SH-SY5Y cells in the absence (CTRL) or in the presence of ACTZ (2 x 10^{-4} M), BFT (10^{-5} M), RESV (2 x 10^{-4} M), DCP (10^{-12} M), 4AP (10^{-6} M) and DMSO (8.4 x 10^{-12} - 1.7 x 10^{-1} M) were reported. The K^+-currents were recorded in the whole-cell configuration in physiological K^+ ion concentrations. The application of Ba^{2+} ions (5 x 10^{-3} M) and TEA (5 x 10^{-3} M) in the extracellular solution fully inhibited the K^+-currents. The application of DMSO at percent concentrations used as a co-solvent caused a non-significant reduction in the K^+-currents as determined by student t test ($p > 0.05$). **(B)** Concentration-response relationships of ACTZ, BFT, RESV, DCP and 4AP on whole-cell K^+-currents in SH-SY5Y cells. The concentration-response relationships of the drugs were constructed *vs* DMSO condition at +30 mV (Vm). Each experimental point represents the mean ± S.E. of the percentage of inhibition of K^+-currents *versus* compound concentration of a minimum of five and a maximum of twelve patches. RESV was more effective than the other drugs in reducing the K^+-currents (ANOVA one way $F = 2.2$, $p < 0.05$; Bonferroni's $p < 0.05$).

showing a maximal efficacy of +130 ± 12% and DE50 of 20 x 10^{-6} M (slope = 1) (Figure 5A). The RIL (10^{-4} M) -activated K^+-currents were fully inhibited by IbTX (6 x 10^{-7} M) (Number of cells = 5) (ANOVA one way $F = 3.2$, $p < 0.05$) (Figure 5B).

Expression of BK channel subunits in SH-SY5Y and Neuro2a cells

The hslo1 and beta 4 subunits were detected by conventional PCR reaction in the SH-SY5Y (Figure 6), and in the Neuro2a cells (data not shown). An enhanced expression of the hslo1 subunit in parallel with the large BK current density was found in the SH-SY5Y cells by RT-PCR experiments (Table 2). In contrast, a low expression of the hslo1 subunit in parallel with the low current density was found in the Neuro2a cells (Table 2). A marked reduction of the expression level of the hslo1 subunit was observed in the SH-SY5Y cell 3 days after transfection with

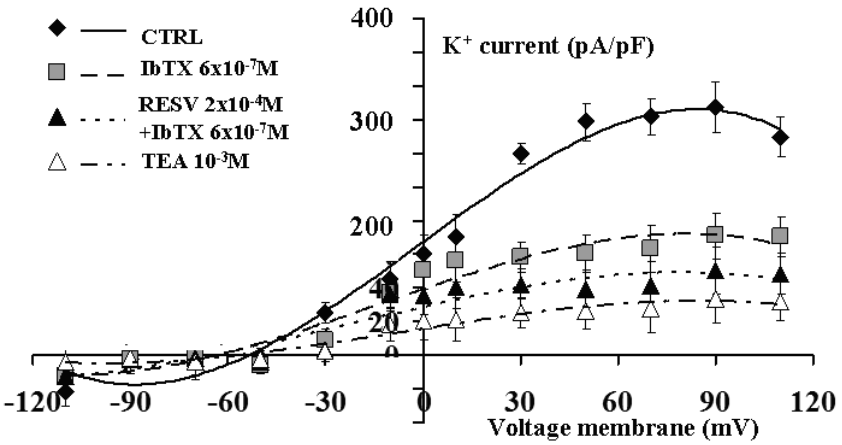

Figure 3. Blocking action of resveratrol (RESV) and iberiotoxin (IbTX) on whole-cell K^+-currents in human SH-SY5Y neuroblastoma cells (cell culture passage 10). I/V relationships of K^+-currents recorded in SH-SY5Y cells in the absence (CTRL) or in the presence of IbTX (6×10^{-7} M), RESV (2×10^{-4} M) + IbTX (6×10^{-7} M) and TEA (10^{-3} M) were reported. The K^+-currents were recorded in a whole-cell configuration in physiological K^+ ion concentrations. The cells (Number of cells = 5) were exposed to control solution (CTRL), IbTX solution, IbTX + RESV solution followed by the application of TEA solution. IbTX reduced the currents with respect to the CTRL. A mild non-significant additional reduction in the current was observed in the presence of RESV with respect to the IbTX currents (ANOVA one way $F = 1.1$, $p > 0.05$).

the anti-KCNMA1 small interference RNA molecule (siRNAhslo1) in parallel with the reduction of the K^+-current density (Table 2). The interference RNA molecule used in our experiments was previously used to induce silencing of the hslo1 gene in the PC3 cells [45].

Effects of Kv/BK modulators on cell proliferation in SH-SY5Y and Neuro2a cells

IbTX (6×10^{-7} M) caused a marked reduction in the cell number evaluated using cell dehydrogenase activity (CDA) assay and the impedentiometric assay in the SH-SY5Y cells after 6 h of incubation time, while it failed to affect the cell number in the Neuro2a cells (Table 2). RESV (10^{-4} M) instead caused a significant reduction in the cell number in SH-SY5Y and Neuro2a cells being, however more effective in the SH-SY5Y (Table 2).

The effects of RESV (10^{-7} - 2×10^{-4} M) on CDA of SH-SY5Y cells were concentration-dependent, decreasing it after 3 h (ANOVA one way $F = 19.02$, $p < 0.05$; Bonferroni's $p < 0.05$), 6 h (ANOVA one way $F = 11.2$, $p < 0.05$; Bonferroni's $p < 0.05$) and 24 h of incubation time with respect to the DMSO condition (ANOVA one way $F = 12.01$, $p < 0.05$; Bonferroni's $p < 0.05$). The effects of IbTX (10^{-9} - 6×10^{-7} M) on CDA of SH-SY5Y cells were concentration-dependent, significantly reducing CDA after 6 h of incubation time with respect to the DMSO condition (ANOVA one way $F = 8.2$, $p < 0.05$; Bonferroni's $p < 0.05$) (Figure 7).

RESV affected cell morphology increasing the cell volume evaluated using the impedentiometric assay. The large variance ratio calculated at 3 h and 6 h was indeed due to RESV (10^{-4} M) (Bonferroni's $p < 0.05$) that enhanced cell diameter and volume, and reduced cell number, and IbTX (6×10^{-7} M) that reduced cell number at 6 h (Bonferroni's $p < 0.05$) (ANOVA one way $F = 8.3$ at 3 h, $F = 6.2$ at 6 h, $p < 0.05$) (Figure 8).

RIL (5×10^{-5} - 10^{-4} M) also caused a significant and concentration-dependent decrease in CDA after 6 h (Bonferroni's $p < 0.05$) and 24 h (Bonferroni's $p < 0.05$) of incubation time with respect to the DMSO condition. The percent change in CDA was linearly correlated with RESV ($R = 0.891$) and RIL ($R = 0.921$) concentrations. TEA (10^{-6} - 10^{-3} M) induced a non-significant change in this parameter with respect to the control condition (ANOVA one way $F = 1.01$, $p > 0.05$) (Figure 7).

The incubation of the cells over a period of 3 h, 6 h and 24 h with ACTZ (10^{-7} - 2×10^{-4} M),

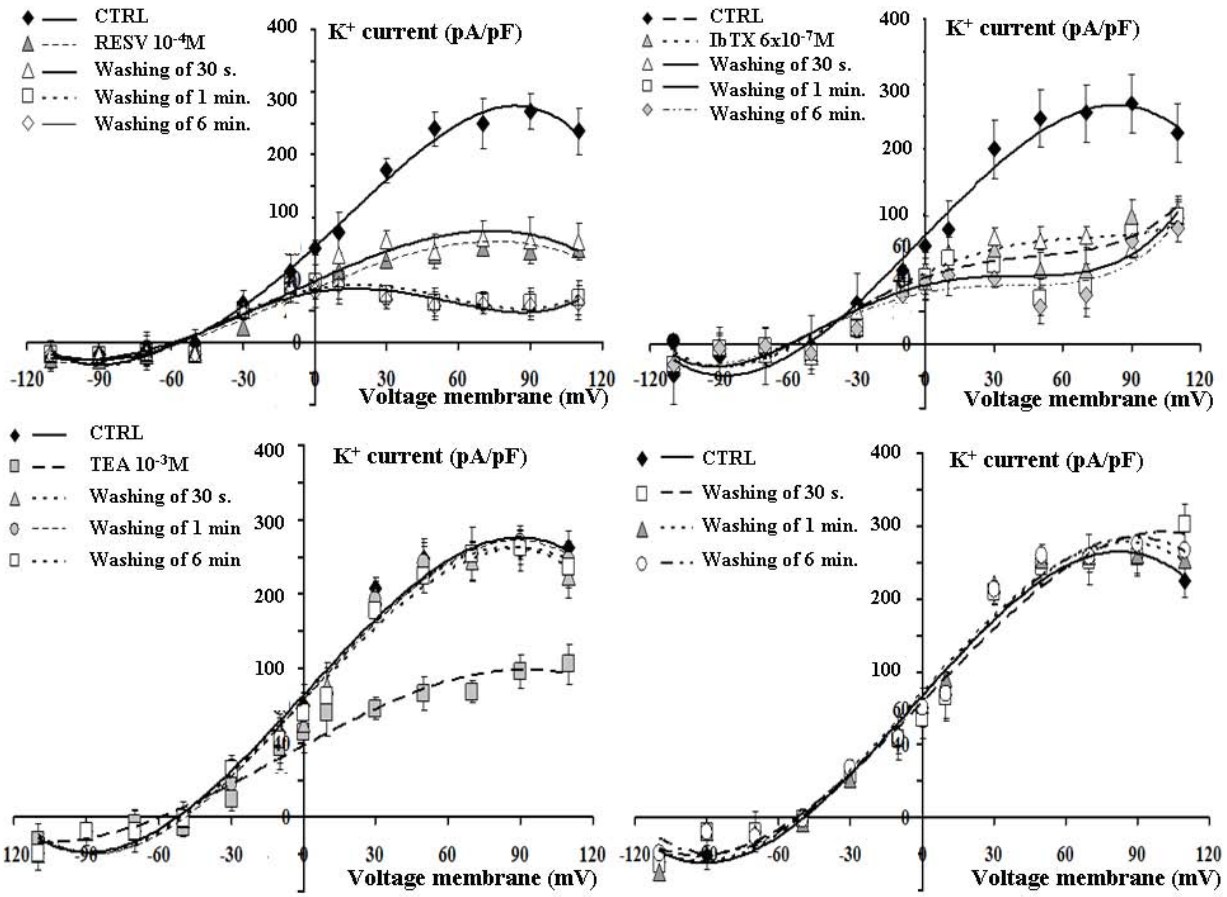

Figure 4. Current/voltage relationships recorded in human SH-SY5Y neuroblastoma cells at different washing times of bath solutions (cell culture passage 10). The K^+-currents were recorded in a whole-cell configuration in physiological K^+ ion concentrations. The cells were perfused with the solutions for 1 min before recording and the currents were recorded in the presence of resveratrol (RESV) (10^{-4} M), iberiotoxin (IbTX) (6 x 10^{-7} M), tetraethylammonium (TEA) (10^{-3} M) and bath solution (CTRL). No significant changes in the K^+-current recorded at +30 mV (Vm) were observed between TEA (10^{-3} M) and CTRL after 6 min of washout (t test $p > 0.05$). A significant difference was calculated between RESV and IbTX data *vs* CTRL solution (t test $p < 0.05$).

BFT (10^{-9} - 10^{-5} M), DCP (10^{-12} - 2 x 10^{-4} M) and 4AP (10^{-8} - 10^{-4} M) did not change the CDA significantly with respect to the DMSO condition of either SH-SY5Y and Neuro2a cells (data not shown).

Moreover, ACTZ (2 x 10^{-4} M), BFT (10^{-5} M), DCP (2 x 10^{-4} M), 4AP (10^{-7} M - 10^{-4} M) and RIL (10^{-6} M - 10^{-4} M) failed to affect cell morphology and number of SH-SY5Y cells (Figure 8), and Neuro2a cells (data not shown).

RESV (10^{-4} M) (student t test $p < 0.05$) and IbTX (6 x 10^{-7} M) (student t test $p < 0.05$) significantly reduced the surviving fraction of the clone with respect to DMSO conditions of the clonogenic assay (Figure 9). No significant effects were observed with ACTZ, BFT, DCP, 4AP, RIL and TEA on cell survival.

The role of BK channels in the proliferation of neuroblastoma cells was further substantiated by gene-specific mRNA silencing using RNA interference (RNA_i). The anti-KCNMA1 small interference RNA molecule (siRNAhslo1) was transfected into SH-SY5Y cells, which significantly reduced KCNMA1 mRNA expression and cell proliferation after three days of the transfection. The siRNAhslo1 significantly inhibited mRNA expression, cell proliferation and whole-cell K^+-current, when compared to non-transfected cells (control cells) (Table 2).

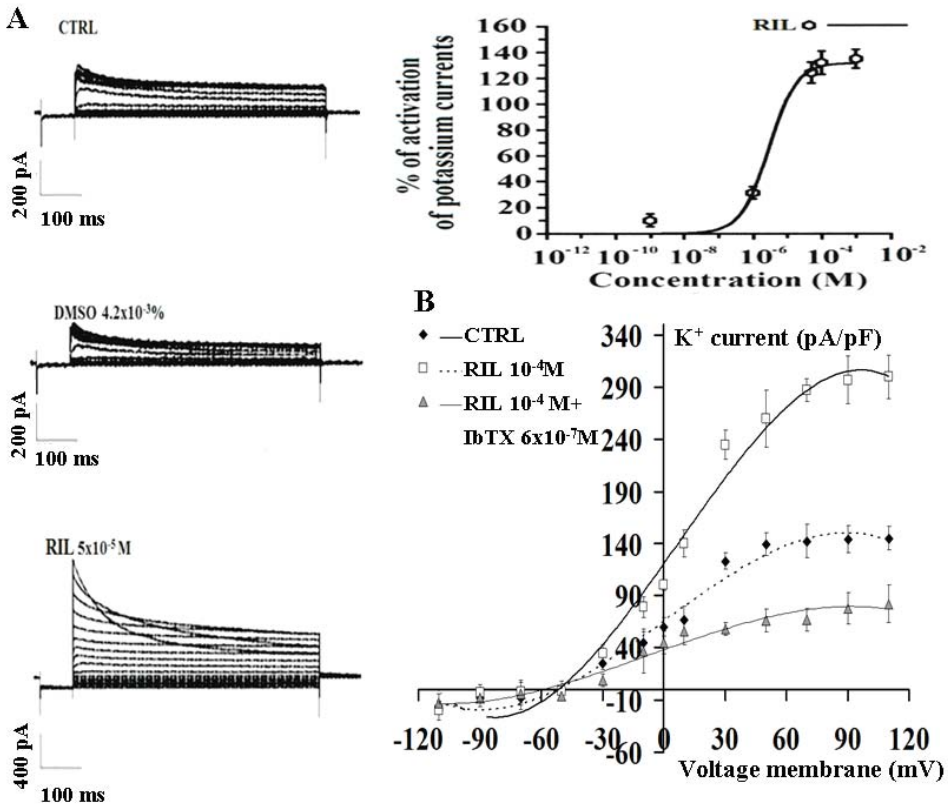

Figure 5. Activating action of riluzole (RIL) on whole-cell K^+-currents in human SH-SY5Y neuroblastoma cells (cell culture passage 10). Sample traces of K^+-currents recorded in the absence (CTRL) or in the presence of RIL (10^{-4} M) were reported. The K^+-currents were recorded in a whole-cell configuration in physiological K^+ ion concentrations. (**A**) RIL was effective in inducing activation of K^+-currents. The application of DMSO at percent concentrations used as a co-solvent caused a non-significant reduction of the K^+-currents. The concentration-response relationship of the RIL was constructed *vs* DMSO condition at +30 mV (Vm). Each experimental point represents the mean ± S.E. of the percentage of inhibition of K^+-currents *versus* compound concentration of a minimum of five and a maximum of six patches. (**B**) I/V relationship of K^+-currents recorded in the absence (CTRL) or in the presence of RIL (10^{-4} M) and RIL (10^{-4} M) + IbTX (6×10^{-7} M) were reported (ANOVA one way $F = 3.2$, $p < 0.05$). The data showed the RIL-activated current was fully inhibited by IbTX.

In whole-cell patch clamp experiments, inhibition of the membrane conductance by IBTX and RESV was almost abolished in RNA_i-treated cells. IbTX failed to affect cell proliferation in the impedentiometric and enzymatic assays, while RESV reduced cell number being, however less effective in the RNA_i-treated cells with respect to the control cells (Table 2).

The involvement of inwardly rectifying K^+ (Kir) channels in the regulation of cell proliferation was investigated in neuroblastoma cell lines. The Kir channel blocker Ba^{2+} ions ($1 - 5 \times 10^{-4}$ M), the KATP-channel blocker glibenclamide (1×10^{-9} M, 100×10^{-9} M) and the KATP-channel opener diazoxide (250×10^{-9} M, 200×10^{-6} M) failed to affect CDA, cell volume and diameter within 24 h of incubation time (data not shown). The lack of effects of modulators of inwardly rectifying K^+-channels on the investigated parameters suggest that these channels may not contribute to cell proliferation in these cells.

DISCUSSION

In undifferentiated SH-SY5Y cells, the whole-cell K^+-current recorded in physiological conditions is sustained by the BK channel with a minor contribution of SK channels or other Kv channels. In contrast, the whole-cell K^+-current was

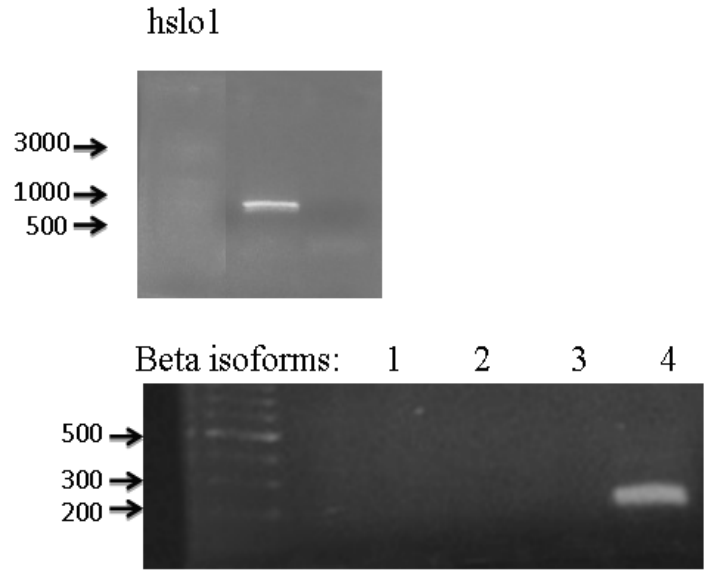

Figure 6. Polymerase Chain Reactions of BK subunits in human SH-SY5Y neuroblastoma cells (cell culture passage 10). Representative agarose gel of amplicons generated from PCR cells show the presence of the full length of the hslo1 and of the beta 4 subunit.

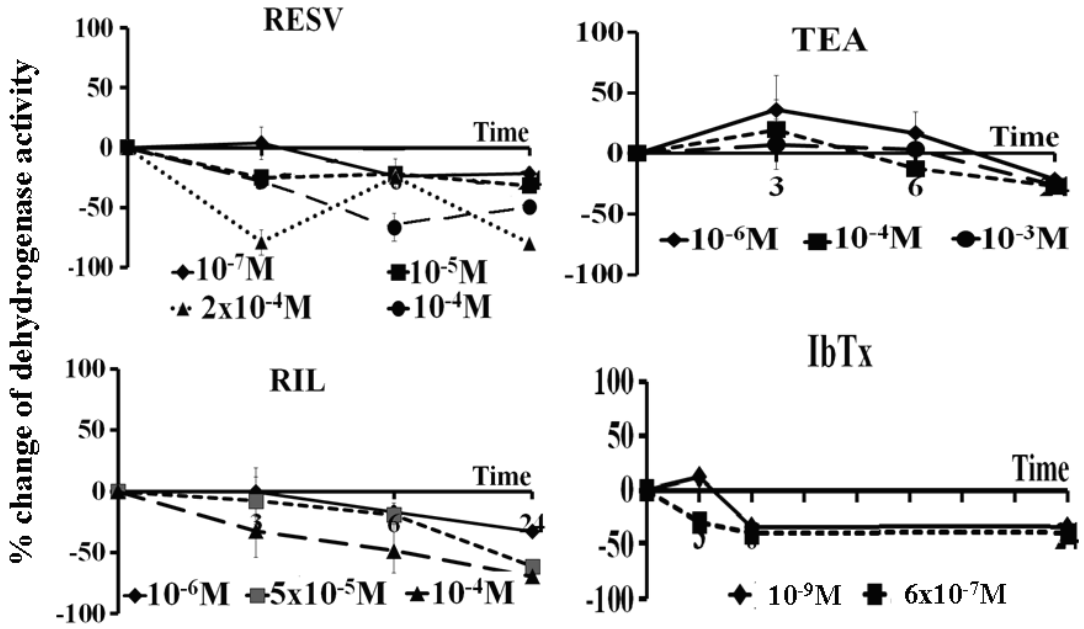

Figure 7. Percentage changes of dehydrogenases activity *vs* control or DMSO condition in the presence of resveratrol (RESV), riluzole (RIL), iberiotoxin (IbTX) and tetraethylammonium (TEA) in SH-SY5Y human neuroblastoma cells (cell culture passage 10). Dehydrogenases activity was measured by using a colorimetric assay (Cell Counting Kit-8, Enzo Life Sciences International, Inc, USA) after the incubation of the cells over a period of 3 h, 6 h and 24 h with RESV (10^{-7}-2 x 10^{-4} M), RIL (5 x 10^{-5} - 10^{-4} M), IbTX (10^{-9} M - 6 x 10^{-7} M) and TEA (10^{-6} - 10^{-3} M). Each experimental point represents the mean ± S.E. of the percentage of dehydrogenases activity *vs* control or DMSO condition of three replicates. These drugs significantly reduced the cell dehydrogenases activity over a period of 24 h (ANOVA one way, $p < 00.5$), except TEA.

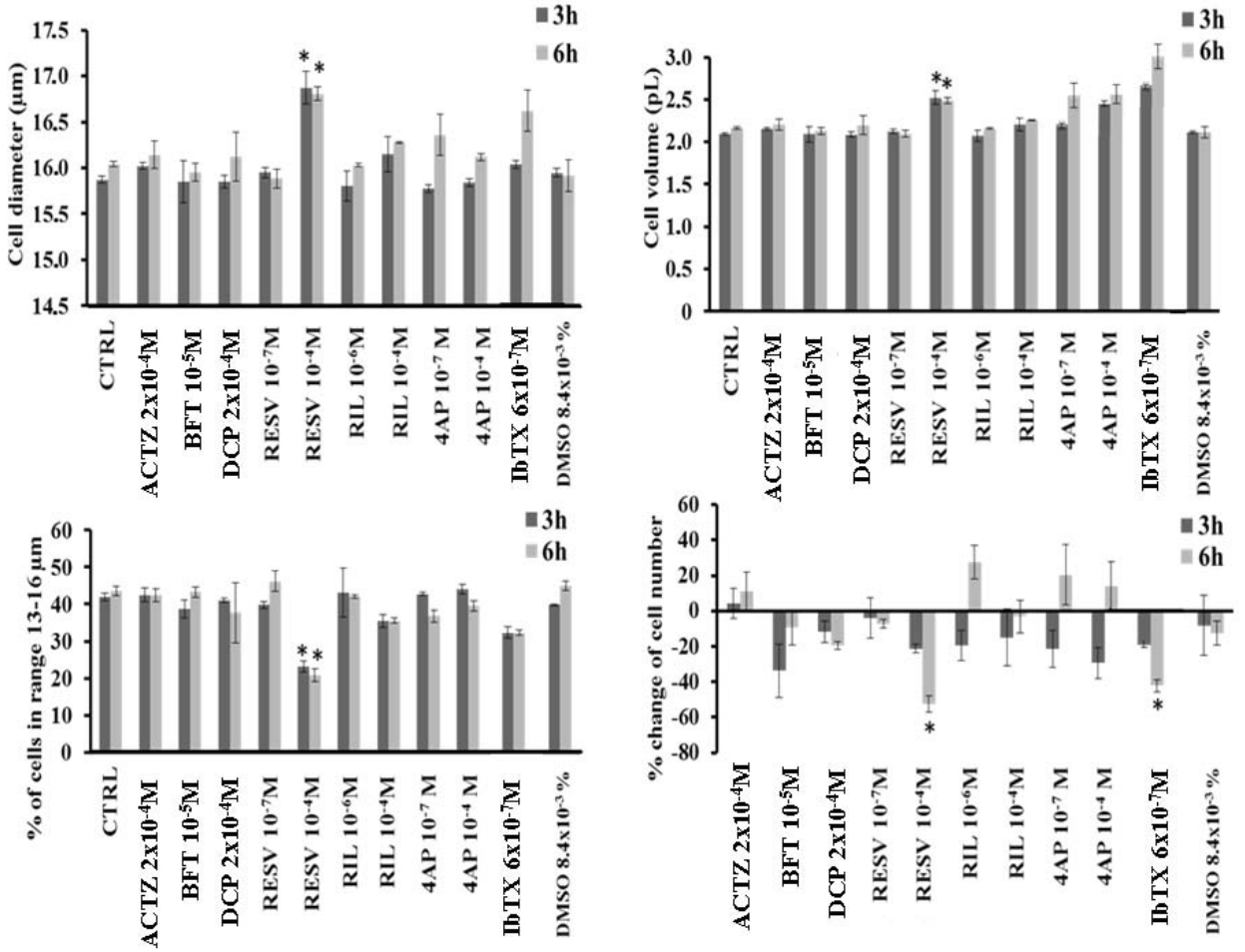

Figure 8. Effects of acetazolamide (ACTZ), bendroflumethiazide (BFT), dichlorphenamide (DCP), 4-aminopyridine (4AP), resveratrol (RESV), iberiotoxin (IbTX), DMSO and riluzole (RIL) on cell morphology and cell number in human SH-SY5Y neuroblastoma cells (cell culture passage 10). The effects of ACTZ (2 x 10^{-4} M), BFT (10^{-5} M), DCP (2 x 10^{-4} M), 4AP (10^{-7} M - 10^{-4} M), RIL (10^{-7} M - 10^{-6} M), IbTX (6 x 10^{-7} M), DMSO (8.4 x 10^{-3} M) and RESV (10^{-7} M - 10^{-4} M) on cell diameter, cell volume and number were evaluated by measuring the voltage changes associated with cell volume changes by using the Scepter™2.0 cell counter (MERK-Millipore, USA) after 3 h and 6 h of incubation time. RESV induced a significant enhancement of the cell diameter and volume, also significantly reducing cell number after 3 h and 6 h of incubation time (ANOVA one way F = 8.3 at 3 h, F = 6.2 at 6 h $p < 0.05$; Bonferroni's $p < 0.05$*). IbTX reduced the cell number after 6 h of incubation (Bonferroni's $p < 0.05$*). Each experimental point represents the mean ± S.E. of three replicates.

markedly lower in the Neuro2a cells and was not sustained by BK channel. The observed mild response of the K^+-currents to 4AP (5 x 10^{-4} M) in our experiments suggests that a specific Kv subtype, such as the Kv4 may contribute only marginally to the total current in the SH-SY5Y cells as previously suggested [46]. We found that the K^+-channel modulators tested in our experiments showed different effects on the whole-cell K^+-currents recorded in SH-SY5Y cells. The most effective inhibitors were TEA, RESV and IbTX, while ACTZ, DCP and BFT showed a partial inhibitory response. The rank order of efficacy as K^+-current inhibitors at +30 mV (Vm) was: TEA > RESV $\geq$ IbTX > DCP > ACTZ > BFT $\geq$ 4AP.

The inhibitory actions of RESV and IbTX of the BK channel current were however not reversible. In contrast, the TEA inhibitory action of the K^+-current was rapidly reversible.

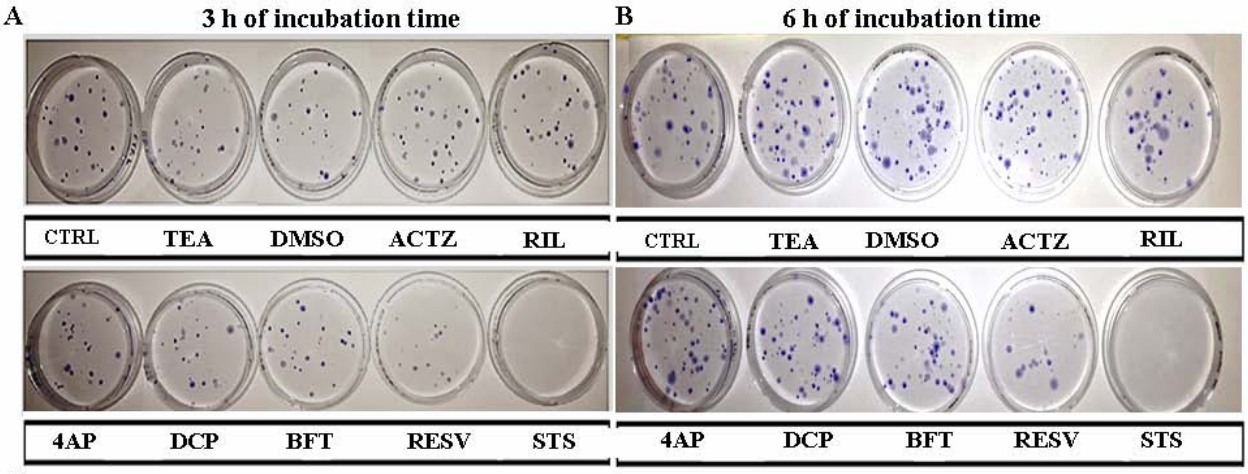

C 3 h of incubation time

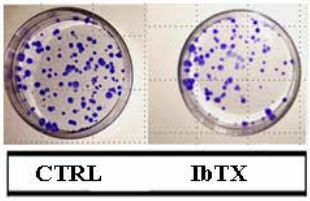

6 h of incubation time

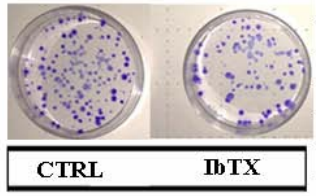

Experimental condition	Surviving fraction 3h(%)	Radius of colonies 3h(pixel)	Surviving fraction 6h(%)	Radius of colonies 6h(pixel)
CTRL	100	9.1±0.34	100	9.03±0.55
4AP 10^{-4}M	81.90±0.03	8.59±0.32	93.98±0.01	9.78±0.05
BFT 10^{-5}M	84.76±0.07	8.39±0.23	95.49±0.05	9.26±0.02
DCP $2x10^{-4}$M	97.14±0.07	7.75±0.21	88.72±0.03	9.15±0.02
DMSO $8.4x10^{-3}$%	83.81±0.01	7.97±0.23	90.98±0.05	9.24±0.20
ACTZ $2x10^{-4}$M	101.90±0.07	8.67±0.29	77.44±0.03	9.52±0.01
RIL 10^{-4}M	80.00±0.09	8.47±0.26	93.23±0.08	9.15±0.63
RESV 10^{-4}M	48.57±0.02 *°	8.05±0.24	39.10±0.03 *°	9.62±0.71
TEA 10^{-3}M	90.48±0.14	7.86±0,20	93.98±0.02	9.81±0.36
IbTX $6x10^{-7}$ M	71.31±0.05	7.52±0.56	50.27±0.073 *°	7.26±0.45

Figure 9. Effects of acetazolamide (ACTZ), bendroflumethiazide (BFT), dichlorphenamide (DCP), 4-aminopyridine (4AP), resveratrol (RESV), riluzole (RIL), iberiotoxin (IbTX), DMSO, and tetraehylammonium (TEA) on cell survival in human SH-SY5Y neuroblastoma cells (cell culture passage 10). The effects of ACTZ (10^{-7} M), BFT (10^{-9} M), DCP (10^{-12} M), 4AP (10^{-4} M), RIL (10^{-4} M), RESV (10^{-4} M), IbTX (6 x 10^{-7} M), DMSO (8.4 x 10^{-3} M) and TEA (10^{-3} M) on cell survival were evaluated after (**A**) 3 h and (**B**) 6 h of incubation time by using the clonogenic assay. RESV induced a significant reduction in the cell clone numbers after 3 h and 6 h of incubation time with respect to control* and DMSO° conditions (student t test $p < 0.05$). (**C**) IbTX also significantly reduced the cell clone numbers after 6 h of incubation time with respect to control and DMSO (student t test $p < 0.05$*,°). Staurosporine (STS) fully reduced clone numbers. Each experimental point represents the mean ± S.E. of three replicates.

A point of interest is the finding that the BK channels can be activated by ACTZ, DCP, RESV and BFT in skeletal muscle and in HEK293 cell expressing the recombinant hslo1 subunit and by RESV in neurons [7, 12, 26, 38], however no activating actions were observed in the undifferentiated SH-SY5Y cells. The lack of activating action of K^+-currents by ACTZ, DCP and BFT in the SH-SY5Y cells can be related to the different molecular composition of the BK channel in these cells. The BK channel functionally active in the SH-SY5Y is composed by the combination of the hslo1 subunit and the β4 subunit which is a neuronal beta subunit [47, 48]. BK channels are indeed composed by the alpha subunit encoded by the *slo1/KCNMA1* gene assembled as tetramer and beta subunits (beta1-4) encoded by *KCNMB1-4* genes. The alpha, alpha+beta 1, alpha+beta 2/3, and beta 4 mimics the skeletal muscle, vascular smooth muscle and neuronal BK channels, respectively [47]. Furthermore, splicing isoforms of the alpha

subunit gene are expressed in the tissues including skeletal muscle affecting physiological properties and pharmacological response of the native channels [40, 49]. The recently cloned gamma subunits contribute to enhance the complexity of BK channels [9].

Riluzole was the only drug in our experiments capable of enhancing the K^+-currents and this effect is related to the activation of the BK channel as supported by the findings in our experimental condition that the riluzole-activated currents were fully inhibited by IbTX. RIL at the same concentrations that reduced cell dehydrogenase activity did not affect the cell morphology and the number and failed to affect the cell surviving fraction in the impedentiometric and clonogenic assays, respectively. These findings suggest that the RIL-dependent activating action of BK channel could have counterbalanced the expected anti-proliferative action of this drug. It should be stressed that riluzole has multiple targets of action, blocking the voltage-dependent sodium and N/P/Q-type calcium channels and activating SK channels [20-23].

In SH-SY5Y cells, both RESV and IbTX concentration-dependently reduced cell dehydrogenase activity, reduced the cell number and the colony surviving fraction in the impedentiometric and clonogenic assays, however RESV being more effective than IbTX. RESV was also effective as an anti-proliferative drug in the Neuro2a cell showing a constitutive low expression/activity of BK channel. These findings indicate that other than the BK-mediated mechanism, additional anti-proliferative mechanisms are involved in the observed effect of RESV. This is further supported by the fact that RESV also shows a significant anti-proliferative action in the RNA_i-treated cells where the expression/activity of the hslo1 subunit is almost absent. The marked K^+-current inhibition exerted by RESV may lead to accumulation of intracellular K^+ ions with cell volume enlargement as observed in our experiments.

IbTX was effective as an anti-proliferative drug in SH-SY5Y cells showing an elevated expression/ activity of the hslo1 subunit, but not in the RNAi-treated cells or in Neuro2a showing a low/ expression activity of the hslo1 subunit.

The anti-proliferative actions of RESV can also be explained by the fact that it can be capable of permeating cell membranes while IbTX is a relatively impermeant toxin and its effects can be associated with the interaction with other targets, the mitochondrial (mito-BK) channels, for instance. BK channel can be located also in the several intracellular compartments, among these the inner mitochondrial membrane [50]. The mito-BK variant has been proposed to be coupled to the respiratory chain complex potentially affecting mito-dehydrogenases activity [51]. The mito-BK channel is composed of a splice variant known as BK-DEC (BK-DEC is harbouring an amino acid sequence of 50AA at the COOH-terminus) and the beta 4 subunit with a minor contribution of the beta 2. The mito-BK channel activation exerts a cytoprotective action on cardiomyocites and neurons [50]. Furthermore, RESV may lead to downregulation of the Akt signaling in neuroblastoma cells [32], and BK channel is coupled with kinases relevant to cell death and survival, like Akt, glycogen synthase kinase-3β and phosphoinositide-dependent kinase-1, thereby contributing to the anti-proliferative effects observed in our experiments [52].

CONCLUSION

Our data are in line with the hypothesis that an elevated expression/activity of the hslo1 subunit is associated with proliferation in the SH-SY5Y cell as observed in non-metastatic (MCF-7) breast cancer cells [53], brain-specific metastatic (MDA-MB-361) breast cancer cells [54], human prostate cancer and glioma [45, 55]. In contrast, some others suggested that BK channel activation has been reported to show anti-proliferative properties in osteosarcoma cells, ovarian cancer cells, glioma cells and in MDA-MB-231 breast cancer cells [14, 56, 57].

Therefore, RESV shows an anti-proliferative action interacting with multiple targets including BK channel. Cells overexpressing BK channels maybe more sensitive to this drug. Whereas acetazolamide and structurally related drugs were not capable of exerting significant effects on cell proliferation in both SH-SY5Y and Neuro2a neuroblastoma cells.

ACKNOWLEDGEMENTS

This work was supported by MIUR (Italian Ministry for Education, University and Research) and the "PON Ricerca e Competitivita' 2007-2013 - Azione I - Interventi di rafforzamento strutturale" PONa3_00052, Avviso 254/Ric; and by "Fondi Ateneo 2012-14 Univ. of Bari, Italy. This work was also supported by "Consorzio Interuniversitario di Ricerca in Chimica dei Metalli nei Sistemi Biologici" Sede legale Piazza Umberto I, Bari 1-70121.

CONFLICT OF INTEREST STATEMENT

The authors declare that the research was conducted in the absence of any commercial or financial relationships that could be construed as a potential conflict of interest.

REFERENCES

1. Tricarico, D., Capriulo, R. and Camerino, D. C. 2002, Neuromuscul. Disord., 12(3), 258.
2. Tricarico, D., Mele, A. and Conte Camerino, D. 2005, Neurobiol. Dis., 20(2), 296.
3. Henney, N. C., Li, B., Elford, C., Reviriego, P., Campbell, A. K., Wann, K. T. and Evans, B. A. 2009, Am. J. Physiol. Cell Physiol., 297(6), C1397-408. doi:10.1152/ajpcell.00311.2009. Epub. 2009, Sep. 23.
4. Park, J. H., Park, S. J., Chung, M. K., Jung, K. H., Choi, M. R., Kim, Y., Chai, Y. G., Kim, S. J. and Park, K. S. 2010, Biochem. Biophys. Res. Comm., 396, 637-642.
5. Chang, H., Ma, Y. G., Wang, Y. Y., Song, Z., Li, Q., Yang, N., Zhao, H. Z., Feng, H. Z., Chang, Y. M., Ma, J., Yu, Z. B. and Xie, M. J. 2011, J. Cell Physiol., 226(6), 1660-1675. doi:10.1002/jcp.22497.
6. Jia, X., Yang, J., Song, W., Li, P., Wang, X., Guan, C., Yang, L., Huang, Y., Gong, X., Liu, M., Zheng, L. and Fan, Y. 2013, Pflügers Arch., 465(2), 221-232. doi:10.1007/s00424-012-1182-z. Epub. 2012, Nov. 21.
7. Tricarico, D., Mele, A., Calzolaro, S., Cannone, G., Camerino, G. M., Dinardo, M. M., Latorre, R. and Conte Camerino, D. 2013, PLoS One, 7, 16.
8. Curci, A., Mele, A., Camerino, G. M., Dinardo, M. M. and Tricarico, D. 2014, Front. Physiol., 5, 476. doi:10.3389/fphys.2014.00476. eCollection.
9. Toro, L., Li, M., Zhang, Z., Singh, H., Wu, Y. and Stefani, E. 2014, Pflügers Arch – Eur. J. Physiol., 466, 875-886. doi:10.1007/s00424-013-1359-0.
10. Pierno, S., Tricarico, D., Liantonio, A., Mele, A., Digennaro, C., Rolland, J. F., Bianco, G., Villanova, L., Merendino, A., Camerino, G. M., De Luca, A., Desaphy, J. F. and Camerino, D. C. 2014, Age (Dordr), 36(1), 73. doi:10.1007/s11357-013-9544-9.
11. Gribkoff, V. K., Starrett, J. E. Jr. and Dworetzky, S. I. 2001, Neuroscientist, 7(2), 166-77.
12. Tricarico, D., Barbieri, M., Mele, A., Carbonara, G. and Camerino, D. C. 2004, FASEB J., 18(6), 760-761.
13. Tricarico, D., Mele, A. and Conte, C. D. 2006, Neuromuscul. Disord., 16(1), 39-45.
14. Ma, Y. G., Liu, W. C., Dong, S., Du, C., Wang, X. J., Li, J. S., Xie, X. P., Wu, L., Ma, D. C., Yu, Z. B. and Xie, M. J. 2012, PLoS One, 7(5), e37451. doi:10.1371/journal.pone.0037451.
15. Bentzen, B. H., Olesen, S. P., Rønn, L. C. and Grunnet, M. 2014, Front. Physiol., 5, 389. doi:10.3389/fphys.2014.00389.
16. Tricarico, D., Montanari, L. and Conte Camerino, D. 2003, Neuromuscul. Disord., 13(9), 712.
17. Tricarico, D., Mele, A., Liss, B., Ashcroft, F. M., Lundquist, A. L., Desai, R. R., George, A. L. Jr. and Conte Camerino, D. 2008, Neuromuscul. Disord., 18(1), 74.
18. Tricarico, D., Lovaglio, S., Mele, A., Rotondo, G., Mancinelli, E., Meola, G. and Camerino, D. C. 2008, Br. J. Pharmacol., 154(1), 183-190. doi:10.1038/bjp.2008.42.
19. Tricarico, D. and Camerino, D. C. 2011, Front. Pharmacol., 2, 8. doi:10.3389/fphar.2011.00008.
20. Huang, C. S., Song, J. H., Nagata, K., Yeh, J. Z. and Narahashi, T. 1997, J. Pharmacol. Exp. Ther., 282, 1280-1290.
21. Zona, C., Siniscalchi, A., Mercuri, N. B. and Bernardi, G. 1998, Neurosci., 85, 931-938.
22. Noh, K. M., Hwang, J. Y., Shin, H. C. and Koh, J. Y. 2000. Neurobiol. Dis., 7, 375-383.

23. Dimitriadi, M., Kye, M. J., Kalloo, G., Yersak, J. M., Sahin, M. and Hart, A. C. 2013, J. Neurosci., 33(15), 6557-6562.
24. Robb, E. L. and Stuart, J. A 2010, Molecules, 15, 1196-1212.
25. Rieder, S. A., Nagarkatti, P. and Nagarkatti, M. 2012, Br. J. Pharmacol., 167(6), 1244-1258. doi:10.1111/j.1476-5381.2012.02063.x.
26. Wang, Y. J., Chan, M. H., Chen, L., Wu, S. N. and Chen, H. H. 2016, J. Biomed. Sci., 23(1), 47. doi:10.1186/s12929-016-0259-y.
27. Faes, S., Planche, A., Uldry, E., Santoro, T., Pythoud, C., Stehle, J-C., Horlbeck, J., Letovanec, I., Riggi, N., Datta, D., Demartines, N. and Dormond, O. 2016, Oncotarget, 7(24), 36666-36680. doi:10.18632/oncotarget.9134.
28. Koltai, T. 2016, Onco Targets Ther., 9, 6343-6360. Published online 2016, Oct. 17. doi:10.2147/OTT.S115438.
29. Yu, L. J., Wall, B. A., Wangari-Talbot, J. and Chen, S. 2016, Neuropharmacol., S0028-3908(16), 30046-6. doi:10.1016/j.neuropharm.2016.02.011.
30. Athar, M., Back, J. H., Kopelovich, L., Bickers, D. R. and Kim, A. L. 2009, Arch. Biochem. Biophys., 486(2), 95-102. doi: 10.1016/j.abb. 2009.01.018.
31. Carter, L. G., D'Orazio, A. J. and Pearson, K. J. 2014, Endocr. Relat. Cancer, 21(3), R209-R225. Prepublished online 2014, Feb. 5. doi:10.1530/ERC-13-0171.
32. Graham, R., Hernandez, F., Puerta, N., De Angulo, G., Webster, K. A. and Vanni, S. 2016, Exp. & Mol. Medicine, 48, e210. doi:10.1038/emm.2015.116.
33. Santos, N. C., Figueira-Coelho, J., Martins-Silva, J. and Saldanha, C. 2003, Biochem. Pharmacol., 65, 1035-1041.
34. Jacob, S. W. and de la Torre, J. C. 2009, Pharmacol. Rep., 61, 225-235.
35. Dwane, S., Durack, E. and Kiely, P. A. 2013, BMC Res. Notes, 6, 366. doi: 10.1186/1756-0500-6-366.
36. Tricarico, D., Barbieri, M., Antonio, L., Tortorella, P., Loiodice, F. and Camerino, D. C. 2003, Br. J. Pharmacol., 139(2), 255.
37. Tricarico, D., Mele, A., Camerino, G. M., Laghezza, A., Carbonara, G., Fracchiolla, G., Tortorella, P., Loiodice, F. and Camerino, D. C. 2008, Mol. Pharmacol., 74(1), 50-58. doi:10.1124/mol.108.046615. Epub. 2008, Apr. 10.
38. Tricarico, D., Mele, A., Calzolaro, S., Cannone, G., Camerino, G. M., Dinardo, M. M., Latorre, R. and Conte, C. D. 2013, PLoS One, 8(7), e69551. doi:10.1371/journal.pone.0069551.
39. Mele, A., Buttiglione, M., Cannone, G., Vitiello, F., Camerino, D. C. and Tricarico, D. 2012, Pharmacol. Res., 66(5), 401-408. doi:10.1016/j.phrs.2012.07.007. Epub. 2012, Aug. 9.
40. Dinardo, M. M., Camerino, G., Mele, A., Latorre, R., Conte-Camerino, D. and Tricarico, D. 2012, PLoS One, 7(7), 1-12. e40235. doi:10.1371/journal.pone.0040235. PubMed: 22808126.
41. Tricarico, D., Mele, A., Camerino, G. M., Bottinelli, R., Brocca, L., Frigeri, A., Svelto, M., George, A. L. Jr. and Camerino, D. C. 2010, J. Physiol., 588(Pt. 5), 773. doi:10.1113/jphysiol.2009.185835.
42. Berridge, M. V., Herst, P. M. and Tan, A. S. 2005, Biotechnol. Annu. Rev., 11, 127-152.
43. Franken, N. A., Rodermond, H. M., Stap, J., Haveman, J. and van Bree, C. 2006, Nat. Protoc., 1(5), 2315-2319.
44. Geissmann, Q. 2013, PLoS One, 8(2), e54072. doi:10.1371/journal.pone.0054072. Epub. 2013, Feb. 15.
45. Bloch, M., Ousingsawat, J., Simon, R., Schraml, P., Gasser, T. C., Mihatsch, M. J., Kunzelmann, K. and Bubendorf, L. 2007, Oncogene, 26(17), 2525-2534.
46. Tosetti, P., Taglietti, V. and Toselli, M. 1998, J. Neurophysiol., 79(2), 648-658.
47. Torres, Y. P., Granados, S. T. and Latorre, R. 2014, Front. Physiol., 5, 383. doi: 10.3389/fphys.2014.00383. eCollection 2014.
48. Samengo, I., Currò, D., Barrese, V., Taglialatela, M. and Martire, M. 2014, Neurochem. Res., 39(5), 901-910. doi: 10.1007/s11064-014-1287-1. Epub. 2014, Mar. 26.
49. Shipston, M. J. and Tian, L. 2016, Int. Rev. Neurobiol., 128, 91-126. doi:10.1016/bs.irn.2016.02.012. Epub. 2016, Mar. 3.
50. Balderas, E., Zhang, J., Stefani, E. and Toro, L. 2015, Front. Physiol., 6, 104. doi: 10.3389/fphys.2015.00104.

51. Bednarczyk, P., Wieckowski, M. R., Broszkiewicz, M., Skowronek, K., Siemen, D. and Szewczyk, A. 2013, PLoS One, 8(6), e68125.
52. Sokolowski, B., Orchard, S., Harvey, M., Sridhar, S. and Sakai, Y. 2011, PLoS One, 6(12), e28532. doi:10.1371/journal.pone.0028532. Epub. 2011, Dec. 9. Erratum in: PLoS One, 2012, 7(1). doi:10.1371/annotation/15e95626-9f5c-4882-ba78-826b80c48028.
53. Ouadid-Ahidouch, H. and Ahidouch, A. 2008, J. Membr. Biol., 221(1), 1-6.
54. Khaitan, D., Sankpal, U. T., Weksler, B., Meister, E. A., Romero, I. A., Couraud, P. O. and Ningaraj, N. S. 2009, BMC Cancer, 9, 258. doi:10.1186/1471-2407-9-258.
55. Weaver, A. K., Bomben, V. C. and Sontheimer, H. 2006, Glia, 54(3), 223-233.
56. Cambien, B., Rezzonico, R., Vitale, S., Rouzaire-Dubois, B., Dubois, J. M., Barthel, R. Karimdjee, B. S., Mograbi, B., Schmid-Alliana, A. and Schmid-Antomarchi, H. 2008, Int. J. Cancer, 123, 365-371. doi:10.1002/ijc.23511.
57. Debska-Vielhaber, G., Godlewski, M. M., Kicinska, A., Skalska, J., Kulawiak, B., Piwonska, M., Zablocki, K., Kunz, W. S., Szewczyk, A. and Motyl, T. 2009, J. Physiol. Pharmacol., 60, 27-36.